ISSN: 0256-307X

中国物理快报
Chinese Physics Letters

Volume 30 Number 4 April 2013

A Series Journal of the Chinese Physical Society
Distributed by IOP Publishing

Online: http://iopscience.iop.org/0256-307X
http://cpl.iphy.ac.cn

Chinese Physical Society
Institute of Physics PUBLISHING

CHIN. PHYS. LETT. Vol. 30, No. 4 (2013) 045201

Particle-in-Cell Simulations of Fast Magnetic Reconnection in Laser-Plasma Interaction *

ZHANG Ze-Chen(张泽琛)[1], LU Quan-Ming(陆全明)[1**], DONG Quan-Li(董全力)[2], LU San(卢三)[1], HUANG Can(黄灿)[1], WU Ming-Yu(吴明雨)[1], SHENG Zheng-Ming(盛政明)[3], WANG Shui(王水)[1], ZHANG Jie(张杰)[3]

[1]*CAS Key Lab of Geoscience Environment, University of Science and Technology of China, Hefei 230026*

[2]*School of Physics and Optoelectronic Engineering, Ludong University, Yantai 264025*

[3]*Key Laboratory for Laser Plasmas (MoE) and Department of Physics, Shanghai Jiao Tong University, Shanghai 200240*

(Received 22 October 2012)

Recent experiments have observed magnetic reconnection in laser-produced high-energy-density (HED) plasma bubbles. We perform two-dimensional (2-D) particle-in-cell (PIC) simulations to investigate magnetic reconnection between two approaching HED plasma bubbles. It is found that the expanding velocity of the bubbles has a great influence on the process of magnetic reconnection. When the expanding velocity is small, a single X line reconnection is formed. However, when the expanding velocity is sufficiently large, we can observe a plasmoid in the vicinity of the X line. At the same time, the structures of the electromagnetic field in HED plasma reconnection are similar to that in Harris current sheet reconnection.

PACS: 52.35.Vd, 52.38.−r, 52.65.Rr DOI: 10.1088/0256-307X/30/4/045201

Magnetic reconnection, the topological change of the magnetic field in plasma, plays an important role in the conversion of magnetic energy to plasma energy. It is considered to be related to a great deal of explosive phenomena, such as solar flares,[1−3] magnetospheric substorms,[4−6] sawtooth relaxation in magnetic fusion devices,[7] and even the magnetotail of unmagnetized planets.[8,9] There are numerous direct evidences that support the existence of magnetic reconnection in space observations[10−14] and laboratory experimental devices.[15,16] Hall effect is considered to play an important role during magnetic reconnection in collisionless plasma.[17−20] Recently, it is reported that magnetic reconnection can also occur in laser-produced high-energy-density (HED) plasmas.[21−24] By focusing lasers to small-scale spots on a foil, the foil is ionized and HED plasma bubbles are created. The bubbles expand supersonically off the surface of the foil, and may then be squeezed together. At the same time, a magnetic field with a megagauss order is generated around each bubble. Therefore, a fast reconnection may be observed when two bubbles with opposing magnetic field are squeezed each other. Fox *et al.*[25,26] performed fully kinetic particle-in-cell (PIC) simulations with geometry and parameters relevant to the HED plasma experiments.[21−24] They found that the reconnection rate of magnetic reconnection in HED plasma bubbles is much higher than the prediction of the classic theory. The fast reconnection is caused due to the magnetic flux pileup at the shoulder of the current sheet, and the plasma inflow rate is much larger than the reconnection rate. Then, the subsequent fast reconnection occurs because the reconnection rate is in direct proportion to the square of the amplitude of the magnetic field. In this Letter, by performing two-dimensional (2-D) PIC simulations, we investigate the effects of the expanding velocity on the process of HED plasma reconnection.

In our 2-D PIC simulations, the electromagnetic fields are defined on the grids and updated by solving the Maxwell equations with a full explicit algorithm, and the particles move in the electromagnetic fields. The whole system runs in (x, z) coordinates with the domain size $[-L_x, L_x] \times [-L_z, L_z]$. The system is periodic in both x and z directions. The model of magnetic reconnection between plasma bubbles in this study is based on Refs. [25,26]. Two half-plasma-bubbles are defined on the rectangular area with centers locate at $(0, -L_z)$ and $(0, +L_z)$. The radius vectors of the bubbles are defined from the center of each bubble, which can be expressed as $\boldsymbol{r}^{(1)} = (x, z + L_z)$ and $\boldsymbol{r}^{(2)} = (x, z - L_z)$. The initial number density is $n_\mathrm{b} + n^{(1)} + n^{(2)}$, where n_b is a background density and $n^{(i)}$ (i=1,2) is

$$n^{(i)} = \begin{cases} (n_0 - n_\mathrm{b}) \cos^2\left(\frac{\pi r^{(i)}}{2L_n}\right) & \text{if } r^{(i)} < L_n, \\ 0 & \text{otherwise,} \end{cases} \quad (1)$$

where L_n is the initial scale of the bubbles, and n_0 is the peak bubble density. Initially, the bubbles are ex-

*Supported by the National Natural Science Foundation of China under Grant Nos 11220101002, 41174124, 41274144 and 41121003, the Key Research Program of Chinese Academy of Sciences (KZZD-EW-01), the National Basic Research Program of China (2012CB825602), and the Ocean Public Welfare Scientific Research Project, State Oceanic Administration of China (No 201005017).

**Corresponding author. Email: qmlu@ustc.edu.cn

panding radially, and the velocity is expressed as the sum of the following fields

$$\boldsymbol{V}^{(i)} = \begin{cases} V_0 \sin\left(\frac{\pi r^{(i)}}{L_n}\right)\hat{\boldsymbol{r}}^{(i)} & \text{if } r^{(i)} < L_n, \\ 0 & \text{otherwise.} \end{cases} \quad (2)$$

The magnetic field is initialized as the sum of two toroidal ribbons, with

$$\boldsymbol{B}^{(i)} = \begin{cases} B_0 \sin\left(\frac{\pi(L_n - r^{(i)})}{2L_B}\right)\hat{\boldsymbol{r}} \times \hat{\boldsymbol{y}} \\ \qquad \text{if } r^{(i)} \in [L_n - 2L_B, L_n], \\ 0 \qquad \text{otherwise.} \end{cases} \quad (3)$$

Here B_0 is the initial strength of the magnetic field, and L_B is the half-width of the magnetic ribbons. In order to be consistent with the plasma flow, an initial electric field $\boldsymbol{E} = -\boldsymbol{V} \times \boldsymbol{B}$ is added, while the initial out-of-plane current density is determined by Faraday's law.

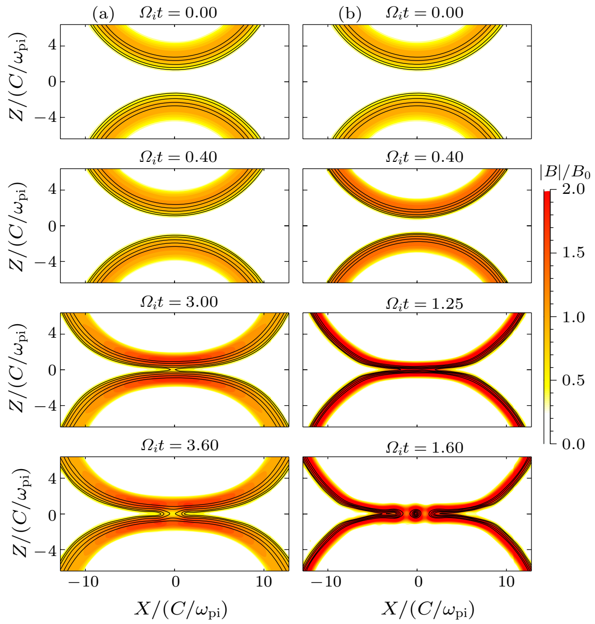

Fig. 1. The evolution of the magnetic field for cases (a) $V_0 = 2.0V_{\rm A}$ at $\Omega_i t = 0$, 0.4, 3.0, 3.6 and (b) $V_0 = 5.0V_{\rm A}$ at $\Omega_i t = 0$, 0.4, 1.25, 1.6. The magnetic field lines are also plotted in the figure for reference.

In the simulations, the mass ratio m_i/m_e is set to be 100 and the light speed c is $30V_{\rm A}$ (where $V_{\rm A}$ is the Alfven speed based on B_0 and n_0). The initial temperature of the ions are assumed to be the same as that of electrons, $T_{i0} = T_{e0} = 0.056 m_e c^2$. The parameters of the plasma bubbles are chosen based on the Rutherford, Omega and SG-II experiments.[21–26] The initial scale of the bubbles is $L_n = 12c/\omega_{pi}$ and the half-width of the magnetic ribbon is $L_B = 2c/\omega_{pi}$ (c/ω_{pi} is the ion inertial length based on n_0). We choose $n_{\rm b}/n_0 = 0.2$. In general, the expanding velocity $V_0 \sim C_{\rm s}$ (where $C_{\rm s}$ is the sound speed), and the plasma $\beta_0 \sim 10$–100. Therefore, the expanding velocity $V_0 \sim 1$–$10V_{\rm A}$. We set $L_x = 25.6c/\omega_{pi}$ and $L_z = 12.8c/\omega_{pi}$, and number of the grids is $N_x \times N_z = 1024 \times 256$. The time step is $\Omega_i t = 0.001$ ($\Omega_i = eB_0/m_i$ is the ion gyrofrequency). More than 2×10^8 particles per species are employed to stimulate the plasma.

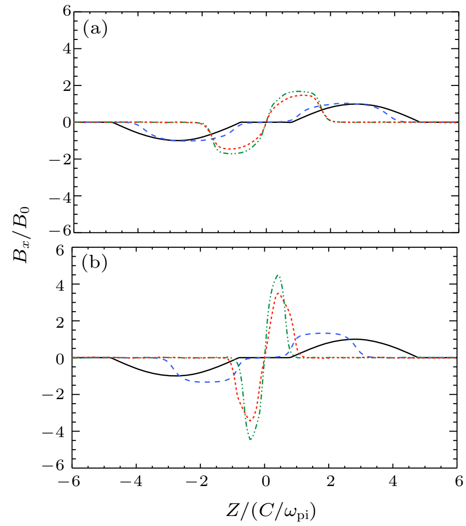

Fig. 2. The magnetic field in the x direction B_x/B_0 along $x = 0$ for the cases (a) $V_0 = 2.0V_{\rm A}$ and (b) $V_0 = 5.0V_{\rm A}$. (a) The black, blue, yellow and red lines represent the time $\Omega_i t$ =0, 0.40, 3.0 and 3.6, respectively. (b) The black, blue, yellow and red lines represent the time $\Omega_i t$ =0.00, 0.40, 1.25 and 1.60, respectively.

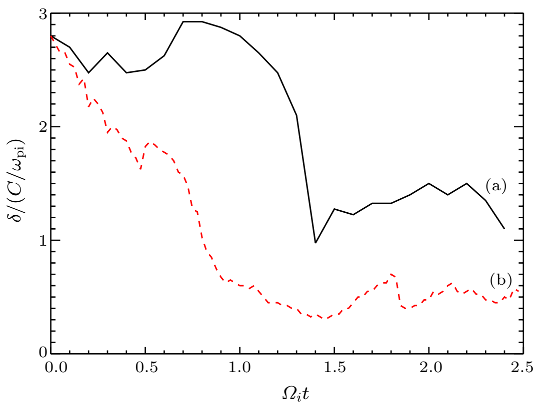

Fig. 3. The evolution of the half-width of the current sheet δ for the cases (a) $V_0 = 2.0V_{\rm A}$ (solid line) and (b) $V_0 = 5.0V_{\rm A}$ (dashed line). The width of the current sheet 2δ is defined as the distance between the positive and negative peaks of B_x along $x = 0$.

In order to investigate the effects of the expanding velocity of the bubbles on the process of HED plasma reconnection, two different values for V_0 are used, which are $2.0V_{\rm A}$ and $5.0V_{\rm A}$, respectively. Figure 1 shows the evolution of the magnetic field for cases (a) $V_0 = 2.0V_{\rm A}$ at $\Omega_i t = 0$, 0.4, 3.0, 3.6 and (b) $V_0 = 5.0V_{\rm A}$ at $\Omega_i t = 0$, 0.4, 1.25, 1.6. The magnetic field lines are also plotted in the figure for reference. As the bubbles approach, an X line is formed at the leading point of the tangency between the bubbles. At the same time, the strong pileup of the magnetic field can be observed in the inflow region, and this is the reason why the reconnection in HED plasma is much faster than that in a Harris current sheet. The reconnection rate is considered to be related to the local Alfven speed in the inflow region, and the pileup of the magnetic field in the inflow region can enhance the local Alfven speed largely. In the case with $V_0 = 2.0V_A$, there is only one X line. However, in the case with $V_0 = 5.0V_A$, a plasmoid appears in the vicinity of the X line during the process of the reconnection. Such a plasmoid has already been observed in the reconnection experiment of laser-plasma interaction.[24] In the experiment, the reconnection occurs between the plasma bubbles with the self-generated magnetic field, where the plasmas are produced by irradiating two laser beams to two suitably juxtaposed Al foil targets. At the same time, the pileup of the magnetic field is much more obvious in the case $V_0 = 5.0V_A$ than in the case $V_0 = 2.0V_A$, therefore the reconnection in the case $V_0 = 5.0V_A$ is much faster.

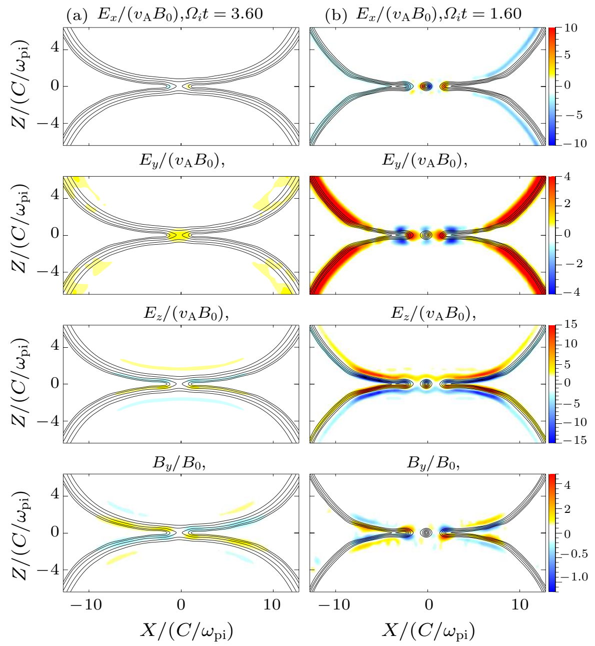

Fig. 4. Contours of the electric field in the x direction $E_x/(V_A B_0)$, the electric field in the y direction $E_y/(V_A B_0)$, the electric field in the z direction $E_z/(V_A B_0)$, and the out-of-plane magnetic field B_y/B_0 for the cases (a) $V_0 = 2.0V_A$ at $\Omega_i t = 3.6$ and (b) $V_0 = 5.0V_A$ at $\Omega_i t = 1.6$, when the reconnection is fully developed.

The pileup of the magnetic field in the inflow region of the reconnection can be observed more clearly in Fig. 2, which shows that the magnetic field in the x direction B_x/B_0 along $x = 0$ for cases (a) $V_0 = 2.0V_A$ and (b) $V_0 = 5.0V_A$. We can find that as the bubbles approach, the magnetic field is enhanced in the inflow region. The enhancement of the magnetic field is more obvious in the case $V_0 = 5.0V_A$. Figure 3 shows the evolution of the half-width of the current sheet δ for the cases (a) $V_0 = 2.0V_A$ and (b) $V_0 = 5.0V_A$. The width of the current sheet 2δ is defined as the distance between the positive and negative peaks of B_x along $x = 0$. The current sheet is squeezed before the reconnection occurs. The width of the current sheet 2δ in the case $V_0 = 5.0V_A$ is much narrower than that in the case $V_0 = 2.0V_A$ when the reconnection occurs. The times, when the reconnection just happens, are about $\Omega_i t = 1.6$ and 0.8 in the cases $V_0 = 2.0V_A$ and $5.0V_A$, respectively, and their corresponding half-widths of the current sheet δ are about 0.6 c/ω_{pi} and $1.2c/\omega_{pi}$. Therefore, multiple X line reconnection occurs in the case $V_0 = 5.0V_A$, and we can observe the plasmoid during the reconnection.

Figure 4 shows the contours of the electric field in the x direction $E_x/(V_A B_0)$, the electric field in the y direction $E_y/(V_A B_0)$, the electric field in the z direction $E_z/(V_A B_0)$, and the out-of-plane magnetic field B_y/B_0 for the cases (a) $V_0 = 2.0V_A$ at $\Omega_i t = 3.6$ and (b) $V_0 = 5.0V_A$ at $\Omega_i t = 1.6$, when the reconnection is fully developed. In the case $V_0 = 2.0V_A$, a single X line reconnection is formed. In the vicinity of the X line, the out-of-plane magnetic field B_y exhibits a quadrupole structure, while E_x forms a bicrescent shape around the X line with a negative value on the left and a positive value on the right. The reconnection electric field E_y points to the y direction, while E_z forms two strips, which points to the center of the current sheet. In the case of $V_0 = 5.0V_A$, a plasmoid is formed in the vicinity of the X line. In the plasmoid, there exists E_x in the left and right parts in the plasmoid, which directs to the center of the plasmoid. E_y in the plasmoid also forms two strips, which points to the center. The structures are similar to that in the Harris current sheet reconnection.[27–32]

In summary, we performed 2-D PIC simulations to investigate magnetic reconnection in two approaching HED, laser produced plasma bubbles. When the expanding velocity of the bubbles is small, a single X line reconnection is formed. However, when the expanding velocity of the bubbles is sufficiently large, we can observe that a plasmoid appears in the vicinity of the X line. A plasmoid has already observed been observed in the reconnection experiment of two approaching HED laser-produced plasma bubbles.[24]

References

[1] Giovanelli R G 1946 *Nature* **158** 81
[2] Masuda S, Kosugi T, Hara H and Ogawara Y 1994 *Nature* **371** 495
[3] Song H Q, Chen Y, Li G, Kong X L and Feng S W 2012 *Phys. Rev.* X **2** 021015
[4] Angelopoulos V, McFadden J P, Larson D, Carlson C W, Mende S B, Frey H, Phan T, Sibeck D G, Glassmeier K H, Auster U, Donovan E, Mann I R, Rae I J, Russell C T, Runov A, Zhou X Z and Kepko L 2008 *Science* **321** 931
[5] Baker D N, Pulkkinen T I, Angelopoulos V, Baumjohann W and McPherron R L 1996 *J. Geophys. Res.* **101** 12975
[6] Nagai T, Fujimoto M, Saito Y, Machida S, Terasawa T, NakamuraR, Yamamoto T, Mukai T, Nishida A and

Kokubun S 1998 *J. Geophys. Res.* **103** 4419

[7] Wesson J 1997 *Tokamaks* (New York: Oxford University Press)

[8] Eastwood J P, Brain D A, Halekas J S, Drake J F, Phan T D, Oieroset M, Mitchell D L, Lin R P and Acuna M 2008 *Geophys. Res. Lett.* **35** L02106

[9] Zhang T L, Lu Q M, Baumjohann W, Russell C T, Fedorov A, Barabash S, Coates A J, Du A M, Cao J B, Nakamura R, Teh W L, Wang R S, Dou X K, Wang S, Glassmeier K H, Auster H U and Balikhin M 2012 *Science* **336** 567

[10] Oieroset M, Phan T D, Fujimoto M, Lin R P and Lepping R P 2001 *Nature* **412** 414

[11] Wang R S, Lu Q M, Guo J and Wang S 2008 *Chin. Phys. Lett.* **25** 3083

[12] Lu Q M, Huang C, Xie J L, Wang R S, Wu M Y, Vaivads A and Wang S 2010 *J. Geophys. Res.* **115** A11208

[13] Wang R S, Lu Q M, Huang C and Wang S 2010 *J. Geophys. Res.* **115** A01209

[14] Nagai T, Shinohara I, Fujimoto M, Matsuoka A, Saito Y and Mukai T 2011 *J. Geophys. Res.* **116** A04222

[15] Ji H T, Yamada M, Hsu S and Kulsrud R 1998 *Phys. Rev. Lett.* **80** 3256

[16] Ono Y, Tanabe H, Li T, Narushima Y, Yamada T, Inomoto M and Cheng C Z 2011 *Phys. Rev. Lett.* **107** 185001

[17] Huang J and Ma Z W 2008 *Chin. Phys. Lett.* **25** 1764

[18] Guo J and Lu Q M 2007 *Chin. Phys. Lett.* **24** 3199

[19] Ren Y, Yamada M, Gerhardt S, Ji H T, Kulsrud R and Kuritsyn A 2005 *Phys. Rev. Lett.* **95** 055003

[20] Malyshkin L 2008 *Phys. Rev. Lett.* **101** 225001

[21] Nilson P M, Willingale L, Kaluza M C et al 2006 *Phys. Rev. Lett.* **97** 255001

[22] Li C K, Seguin F H, Frenje J A, Rygg J R, Petrasso R D, Town R P J, Landen O L, Knauer J P and Smalyuk V A 2007 *Phys. Rev. Lett.* **99** 055001

[23] Zhong J Y, Li Y T, Wang X G et al 2010 *Nat. Phys.* **6** 984

[24] Dong Q L, Wang S J, Lu Q M et al 2012 *Phys. Rev. Lett.* **108** 215001

[25] Fox W, Bhattacharjee A and Germaschewski K 2011 *Phys. Rev. Lett.* **106** 215003

[26] Fox W, Bhattacharjee A and Germaschewski K 2012 *Phys. Plasmas* **19** 056309

[27] Pritchett P L 2001 *J. Geophys. Res.* **106** 3783

[28] Ma Z W and Bhattacharjee A 2001 *J. Geophys. Res.* **106** 3773

[29] Fu X R, Lu Q M and Wang S 2006 *Phys. Plasmas* **13** 012309

[30] Huang C, Lu Q M and Wang S 2010 *Phys. Plasmas* **17** 072306

[31] Zhou M, Deng X H and Huang S Y 2012 *Phys. Plasmas* **19** 042902

[32] Zhang Q H, Dunlop M W and Lockwood M et al 2012 *J. Geophys. Res.* **117** A08205

Chinese Physics Letters

Volume 30 Number 4 April 2013

GENERAL

040201 Parameter Extension and the Quasi-Rational Solution of a Lattice Boussinesq Equation
NONG Li-Juan, ZHANG Da-Jun, SHI Ying, ZHANG Wen-Ying

040301 A Quantum Communication Protocol Transferring Unknown Photons Using Path-Polarization Hybrid Entanglement
Jino Heo, Chang Ho Hong, Jong In Lim, Hyung Jin Yang

040302 From the Anti-Yang Model to the Anti-Snyder Model and Anti-De Sitter Special Relativity
QI Wei-Jun, REN Xin-An

040303 Exact Vortex Clusters of Two-Dimensional Quantum Fluid with Harmonic Confinement
CHONG Gui-Shu, ZHANG Ling-Ling, HAI Wen-Hua

040304 Long-Lived Rogue Waves and Inelastic Interaction in Binary Mixtures of Bose–Einstein Condensates
LIU Chong, YANG Zhan-Ying, ZHAO Li-Chen, YANG Wen-Li, YUE Rui-Hong

040305 Improvement of Controlled Bidirectional Quantum Direct Communication Using a GHZ State
YE Tian-Yu, JIANG Li-Zhen

040501 Semiclassical Ballistic Transport through a Circular Microstructure in Weak Magnetic Fields
ZHANG Yan-Hui, CAI Xiang-Ji, LI Zong-Liang, JIANG Guo-Hui, YANG Qin-Nan, XU Xue-You

040502 Generalized Chaos Synchronization of Bidirectional Arrays of Discrete Systems
ZANG Hong-Yan, MIN Le-Quan, ZHAO Geng, CHEN Guan-Rong

040601 A Potassium Atom Four-Level Active Optical Clock Scheme
ZHANG Sheng-Nan, WANG Yan-Fei, ZHANG Tong-Gang, ZHUANG Wei, CHEN Jing-Biao

040701 A New Mach–Zehnder Interferometer to Measure Light Beam Dispersion and Phase Shift
YANG Xu-Dong

040702 A High Sensitivity Index Sensor Based on Magnetic Plasmon Resonance in Metallic Grating with Very Narrow Slits
XU Bin-Zong, LIU Jie-Tao, HU Hai-Feng, WANG Li-Na, WEI Xin, SONG Guo-Feng

040703 Principal Component Analysis and Minimum Description Length Criterion Based on Through-Wall Image Enhancement
Muhammad Mohsin Riaz, Abdul Ghafoor

THE PHYSICS OF ELEMENTARY PARTICLES AND FIELDS

041201 Finding a Way to Determine the Pion Distribution Amplitude from the Experimental Data
HUANG Tao, WU Xing-Gang, ZHONG Tao

NUCLEAR PHYSICS

042501 Observation of New Isotope ^{131}Ag via the Two-Step Fragmentation Technique
WANG He, N. Aoi, S. Takeuchi, M. Matsushita, P. Doornenbal, T. Motobayashi, D. Steppenbeck, K. Yoneda, K. Kobayashi, J. Lee, LIU Hong-Na, Y. Kondo, R. Yokoyama, H. Sakurai, YE Yan-Lin

042502 The Influence of the Dependence of Surface Energy Coefficient to Temperature in the Proximity Model
M. Salehi, O. N. Ghodsi

ATOMIC AND MOLECULAR PHYSICS

043101 The Hydrogen Molecular Ion in Strong Fields Using the B-Spline Method
ZHANG Yue-Xia, LIU Qiang, SHI Ting-Yun

043102 First Principles Study of Single Wall TiO_2 Nanotubes Rolled by Anatase Monolayers
ZHANG Hai-Yang, DONG Shun-Le

043201 The Probe Transmission Spectra of ^{87}Rb in an Operating Magneto-Optical Trap in the Presence of an Ionizing Laser
LIU Long-Wei, JIA Feng-Dong, RUAN Ya-Ping, HUANG Wei, LV Shuang-Fei, XUE Ping, XU Xiang-Yuan, DAI Xing-Can, ZHONG Zhi-Ping

FUNDAMENTAL AREAS OF PHENOMENOLOGY(INCLUDING APPLICATIONS)

044201 The Collins Formula Applied in Optical Image Encryption
CHEN Lin-Fei, ZHAO Dao-Mu, MAO Hai-Dan, GE Fan, GUAN Rui-Xia

044202 Femtosecond Laser Pulses for Drilling the Shaped Micro-Hole of Turbine Blades
JIA Hai-Ni, YANG Xiao-Jun, ZHAO Wei, ZHAO Hua-Long, DU Xu, YANG Yong

044203 Two-Mode Steady-State Entanglement in a Four-Level Atomic System
PING Yun-Xia, ZHANG Chao-Min, CHEN Guang-Long, ZHU Peng-Fei, CHENG Ze

044204 Time-Grating for the Generation of STUD Pulse Trains
ZHENG Jun, WANG Shi-Wei, XU Jian-Qiu

044205 The High Quantum Efficiency of Exponential-Doping AlGaAs/GaAs Photocathodes Grown by Metalorganic Chemical Vapor Deposition
ZHANG Yi-Jun, ZHAO Jing, ZOU Ji-Jun, NIU Jun, CHEN Xin-Long, CHANG Ben-Kang

044206 Experimental Demonstration of a Low-Pass Spatial Filter Based on a One-Dimensional Photonic Crystal with a Defect Layer
SONG Dong-Mo, TANG Zhi-Xiang, ZHAO Lei, SUI Zhan, WEN Shuang-Chun, FAN Dian-Yuan

044207 Controlling the Spectral Characteristics of Bismuth Doped Silicate Glass Based on the Reducing Reaction of Al Powder
WANG Yan-Shan, JIANG Zuo-Wen, PENG Jing-Gang, LI Hai-Qing, YANG Lu-Yun, LI Jin-Yan, DAI Neng-Li

044208 Double Grating Expanders for Fourth-Order Dispersion Compensation in Chirped Pulse Amplifiers
WANG Cheng, LENG Yu-Xin

044209 A Tunable Blue Light Source with Narrow Linewidth for Cold Atom Experiments
ZHAI Yue-Yang, FAN Bo, YANG Shi-Feng, ZHANG Yin, QI Xiang-Hui, ZHOU Xiao-Ji, CHEN Xu-Zong

044210 The Multi-Scale and the Multi-Fractality Properties of Speckles on Rough Screen Surfaces
ZHANG Mei-Na, LI Zhen-Hua, CHEN Xiao-Yi, LIU Chun-Xiang, TENG Shu-Yun, CHENG Chuan-Fu

044301 The Existence of Simultaneous Bragg and Locally Resonant Band Gaps in Composite Phononic Crystal
XU Yan-Long, CHEN Chang-Qing, TIAN Xiao-Geng

044501 Patterns in a Two-Dimensional Annular Granular Layer
CAI Hui, CHEN Wei-Zhong, MIAO Guo-Qing

044701 The Effect of Micro-ramps on Supersonic Flow over a Forward-Facing Step
ZHANG Qing-Hu, YI Shi-He, ZHU Yang-Zhu, CHEN Zhi, WU Yu

PHYSICS OF GASES, PLASMAS, AND ELECTRIC DISCHARGES

045201 Particle-in-Cell Simulations of Fast Magnetic Reconnection in Laser-Plasma Interaction
ZHANG Ze-Chen, LU Quan-Ming, DONG Quan-Li, LU San, HUANG Can, WU Ming-Yu, SHENG Zheng-Ming, WANG Shui, ZHANG Jie

045202 The Angular Distribution of Optical Emission Spectroscopy from a Femtosecond Laser Filament in Air
SUN Shao-Hua, LIU Xiao-Liang, LIU Zuo-Ye, WANG Xiao-Shan, DING Peng-Ji, LIU Qing-Cao, GUO Ze-Qin, HU Bi-Tao

CONDENSED MATTER: STRUCTURE, MECHANICAL AND THERMAL PROPERTIES

046101 ***In situ* XAFS Investigation on Zincblende ZnS up to 31.7 GPa**
YANG Jun, ZHU Feng, ZHANG Qian, WU Ye, WU Xiang, QIN Shan, DONG Jun-Cai, CHEN Dong-Liang

046102 **High Quality Pseudomorphic $In_{0.24}$ GaAs/GaAs Multi-Quantum-Well and Large-Area Transmission Electro-Absorption Modulators**
YANG Xiao-Hong, LIU Shao-Qing, NI Hai-Qiao, LI Mi-Feng, LI Liang, HAN Qin, NIU Zhi-Chuan

046103 **Dislocation Multiplication by Single Cross Slip for FCC at Submicron Scales**
CUI Yi-Nan, LIU Zhan-Li, ZHUANG Zhuo

046201 **Dynamic Behaviors of Hydrogen in Martensitic T91 Steel Evaluated by Using the Internal Friction Method**
HU Jing, WANG Xian-Ping, ZHUANG Zhong, ZHANG Tao, FANG Qian-Feng, LIU Chang-Song

046202 **CuO Nanoparticle Modified ZnO Nanorods with Improved Photocatalytic Activity**
WEI Ang, XIONG Li, SUN Li, LIU Yan-Jun, LI Wei-Wei

046401 **A Diblock-Diblock Copolymer Mixture under Parallel Wall Confinement**
PAN Jun-Xing, ZHANG Jin-Jun, WANG Bao-Feng, WU Hai-Shun, SUN Min-Na

046601 **A Dynamic-Order Fractional Dynamic System**
SUN Hong-Guang, SHENG Hu, CHEN Yang-Quan, CHEN Wen, YU Zhong-Bo

046801 **The Enhancement of Laser-Induced Transverse Voltage in Tilted $Bi_2Sr_2Co_2O_y$ Thin Films with a Graphite Light Absorption Layer**
YAN Guo-Ying, ZHANG Hui-Ling, BAI Zi-Long, WANG Shu-Fang, WANG Jiang-Long, YU Wei, FU Guang-Sheng

CONDENSED MATTER: ELECTRONIC STRUCTURE, ELECTRICAL, MAGNETIC, AND OPTICAL PROPERTIES

047101 **An Effective Description of Electron Correlation in the Green Function Approach**
LIU Yu-Liang

047201 **Novel Transport Properties in Monolayer Graphene with Velocity Modulation**
SUN Li-Feng, FANG Chao, LIANG Tong-Xiang

047202 **Graphene Quantum Wells and Superlattices Driven by Periodic Linear Potential**
YAN Wei-Xian

047301 **Characteristics of an Indium-Rich InGaN p–n Junction Grown on a Strain-Relaxed InGaN Buffer Layer**
YANG Lian-Hong, ZHANG Bao-Hua, GUO Fu-Qiang

047401 **Electronic Band Structure and Optical Response of Spinel SnX_2O_4 ($X = Mg$, Zn) through Modified Becke–Johnson Potential**
A. Manzar, G. Murtaza, R. Khenata, S. Muhammad, Hayatullah

047501 **Room-Temperature Ferromagnetism in Fe/Sn-Codoped In_2O_3 Powders and Thin Films**
JIANG Feng-Xian, XI Shi-Bo, MA Rong-Rong, QIN Xiu-Fang, FAN Xiao-Chen, ZHANG Min-Gang, ZHOU Jun-Qi, XU Xiao-Hong

047502 **Electric and Magnetic Properties and Magnetoelectric Effect of the $Ba_{0.8}Sr_{0.2}TiO_3/CoFe_2O_4$ Heterostructure Film by Radio-Frequency Magnetron Sputtering**
WANG Ye-An, WANG Yun-Bo, RAO Wei, GAO Jun-Xiong, ZHOU Wen-Li, YU Jun

047503 **Dzyaloshinskii–Moriya Interaction in Spin 1/2 Antiferromagnetic Rings with Nearest Next Neighbor Coupling**
LI Peng-Fei, CAO Hai-Jing, ZHENG Li

047504 **Robust Half-Metallicity and Magnetic Properties of Cubic Perovskite $CaFeO_3$**
Zahid Ali, Iftikhar Ahmad, Banaras Khan, Imad Khan

047701 **A Metal Oxide Heterostructure for Resistive Random Access Memory Devices**
LIAO Zhao-Liang, CHEN Dong-Min

047702 **Direct Piezoelectric Potential Measurement of ZnO Nanowires Using a Kelvin Probe Force Microscope**
WANG Xian-Ying, XIE Shu-Fan, CHEN Xiao-Dong, LIU Yang-Yang

047703 First Principle Study on the Influence of Sr/Ti Ratio on the Atomic Structure and Dislocation Behavior of $SrTiO_3$
GUAN Li, JIA Guo-Qi, ZUO Jin-Gai, LIU Qing-Bo, WEI Wei, GUO Jian-Xin, DAI Xiu-Hong

047901 The Effect of an Incident Electron Beam on the I–V Characteristics of a Au-ZnSe Nanowire-Au Nanostructure
TAN Yu, WANG Yan-Guo

CROSS-DISCIPLINARY PHYSICS AND RELATED AREAS OF SCIENCE AND TECHNOLOGY

048101 The Nature of Stresses in a Giant Static Granular Column
GE Bao-Liang, SHI Qing-Fan, RAM Chand, HE Jian-Feng, MA Shao-Peng

048201 Strong Coupling of Light with Extremely Thin Non-Close-Packing Colloidal Crystals: Experimental and Theoretical Studies
HUANG Zhong, DONG Wen

048501 Optically Modulated Bistability in Quantum Dot Resonant Tunneling Diodes
WENG Qian-Chun, AN Zheng-Hua, HOU Ying, ZHU Zi-Qiang